1 June 2001

ELSEVIER

Optics Communications 192 (2001) 357–363

OPTICS COMMUNICATIONS

www.elsevier.com/locate/optcom

The refractive index of extraordinary ray for $AgGaSe_2$ crystal in 11–16 μm range

Hau-Wei Wang *, Mao-hong Lu

Institute of Electro-optical Engineering, National Chiao-Tung University, 1001 Ta Hsueh Road, Hsinchu 300, Taiwan, ROC

Received 29 January 2001; accepted 19 March 2001

Abstract

The refractive index of $AgGaSe_2$ for extraordinary ray in the 11–16 μm mid-infrared range was measured and an improved Sellmeier equation from 0.85 to the 16 μm wavelength range is proposed.

In this experiment, the mid-infrared radiations of the 11–16 μm wavelength range were mixed with a near-infrared radiation of the 1.7–1.8 μm wavelength range in $AgGaSe_2$ crystal in type II. With the measurement of phase-matching angles the refractive index for extraordinary ray was calculated. The near-infrared radiation was produced by a β-BBO optical parametric oscillator.

PACS: 42.65; 42.70

Keywords: $AgGaSe_2$; Sellmeier equation; Refractive index; Phase-matching; Sum-frequency

1. Introduction

Silver thiogallate crystal ($AgGaSe_2$) is a very useful nonlinear optical material in a wide infrared range from 0.71 to 18 μm, in which it is transparent. Recently, many papers concerning the applications of this crystal on the frequency doubling of the CW [1] and pulsed [2,3] CO_2 laser, optical parametric oscillator (OPO) [4,5], difference-frequency generation [6,7], and IR conversion [8] have been reported.

In our previous work [9], we did an up-conversion experiment, in which mid-infrared radiations of the 11–16 μm wavelength range were mixed with a near-infrared radiation in $AgGaSe_2$ crystal in type I. We found that the measured phase-matching angles for the wavelength longer than 13.5 μm were obviously different from those calculated with the Sellmeier equations given by Kidal and Mikkelsen [10], Bhar [11], Roberts [12] and Harasaki and Kato [13]. With the measured phase-matching angles we calculated the refractive indices of o-ray in the 11–16 μm wavelength range. Combining our results with the Boyd et al.'s data [14] in the 0.85–11 μm wavelength range, we proposed an improved Sellmeier equation for the o-ray refractive index of $AgGaSe_2$ in the 0.85–16 μm range [9]. Unfortunately, in that experiment we could not do a similar measurement in type II phase matching due to the special cutting of the $AgGaSe_2$ crystal. So we could not check the

* Corresponding author. Tel.: +886-3-571-2121; fax: +886-3-571-6631.

E-mail address: adward3@ms4.hinet.net (H.-W. Wang).

0030-4018/01/$ - see front matter
PII: S0030-4018(01)01183-X

refractive index of e-ray in the 11–16 μm wavelength range.

In this experiment, using another $AgGaSe_2$ crystal with different cutting, we measured the type II phase-matching angles in the 11–16 μm wavelength range and calculated the refractive indices of e-ray. In the same way as we did in Ref. [9], we proposed an improved Sellmeier equation of the e-ray refractive index in the 0.85–16 μm range.

2. Experiment

The setup of this experiment is schematically shown in Fig. 1. The measured MIR radiations were generated by the potassium vapor excited on the 4S–8S or 4S–6D two-photon resonance with a pulsed DCM dye laser (Quanta Ray, PDL-1), pumped by a frequency-doubled Nd:YAG pulsed laser (Continuum, Surelite II). These MIR radiations are the amplified spontaneous emissions (ASEs) from the atomic transitions of $8S_{1/2}$–$7P_{1/2,3/2}$ (14.3788 μm, 14.4724 μm), $7P_{3/2,1/2}$–$7S_{1/2}$ (12.4981 μm, 12.5688 μm), $6D_{5/2}$–$7P_{3/2}$ (16.0904 μm), $6D_{3/2}$–$7P_{1/2,3/2}$ (15.9681 μm, 16.0836 μm), and $7P_{3/2,1/2}$–$5D_{3/2,5/2}$ (11.2528 μm, 11.3101 μm), as shown in Fig. 2. The potassium vapor, which generated the MIR emissions, was enclosed in a heat pipe and heated to a temperature about 430°C with 30 cm heated zone. Argon gas of 6.5

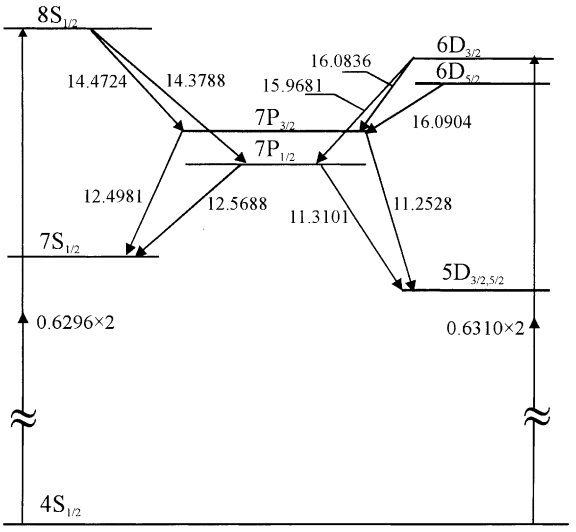

Fig. 2. Partial energy level diagram of potassium showing the related processes in the experiment. All the wavelengths are in μm.

Torr was used as a buffer gas in heat pipe. The entrance window of heat pipe was quartz and the exit window was ZnSe, which can transmit the MIR radiation. Typical operating parameters for the DCM dye laser tuned to a wavelength of 629.6 or 631.0 nm were 6 ns pulse duration, 10 mJ pulse energy, 0.2 cm^{-1} line width, and 10 Hz repetition rate. The dye laser beam was focused by a lens of 100 cm focal length into a spot with a diameter of 0.25 mm at the center of the heat pipe. We put a

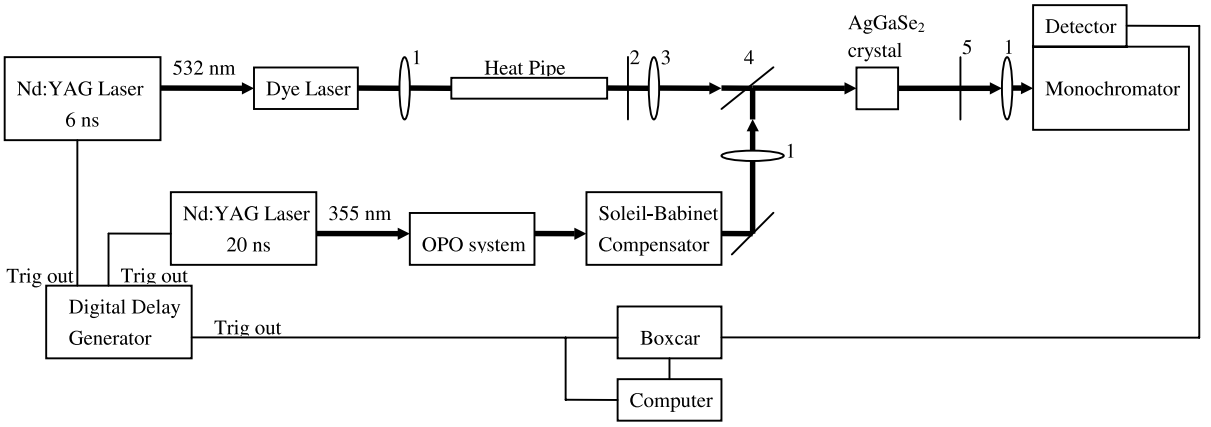

Fig. 1. The setup diagram of this experiment: (1) BK7 lens, (2) Ge mirror, (3) ZnSe lens, (4) 45° dichroic mirror, (5) IR polarizer.

Ge plate behind the heat pipe to blockade the strong DCM dye laser and to transmit the MIR emissions. Since all the MIR emissions were stimulated by the dye laser, we could consider these MIR emissions and the laser beam as collinear. The spot size of the MIR radiation could be considered as same as that of the dye laser, which was about 0.9 mm on the $AgGaSe_2$. The MIR emissions polarized in the crystal principal plane are considered as the extraordinary ray. Here the principal plane is defined as the plane containing the optical axis of crystal and the wave vector of incident beam.

The β-BBO OPO was pumped by a triple-frequency Nd:YAG pulsed laser (Lumonics, HY750) which had 20 ns pulse duration, 43 mJ pulse energy, 0.25 cm^{-1} line width, and 10 Hz repetition rate. The NIR beam of 1.7–1.8 μm from the OPO was used as pumping source for the sum-frequency process and had 1 mm spot size and 0.37 mJ pulse energy on the $AgGaSe_2$ surface. A Soleil–Babinet compensator (Mells Griot Co.) was put in the NIR beam, which converted the polarization of the OPO beam from parallel into perpendicular to the crystal principal plane. The NIR beam was used as o-ray in the sum-frequency process. The NIR beam from OPO and MIR radiations from heat pipe were focused by a BK7 lens of focal length 250 mm and a ZnSe lens of focal length 170 mm respectively, combined together with a 45° dichroic mirror and incident upon the $AgGaSe_2$ crystal.

In order to ensure the temporal overlap of the OPO radiation and the MIR radiation in the crystals, a pulse delay generator was used for the exact timing of the two YAG lasers, as shown in Fig. 1.

The $AgGaSe_2$ crystal, supplied by Physics Institute of the Chinese Academy of Sciences, had dimensions of $7 \times 10 \times 10$ mm^3 with a cut angle of $\theta = 54.4° \pm 0.1°$ and $\phi = 0°$. This cut angle was checked with sum frequency in type II (oe → e) by using the 10.5910 μm CO_2 laser (Edinburgh, PL2) and 1.7850 μm OPO.

We put an IR polarizer behind the $AgGaSe_2$ crystal to blockade the strong OPO beam when the up-converted signal from crystal was measured with a Ge detector (Hamamatsu B1919-01). In all the wavelength measurements a 1 m monochromator (Spex 1704) with a grating of 600 lns/mm was used.

3. Results and discussion

The propagations of the OPO beam and MIR beam in the crystal are shown in Fig. 3. The both beams are mixed in type II (e + o → e). The OPO beam is o-ray and the MIR beam is e-ray in crystal. The measured signals from the $AgGaSe_2$ crystal and the related external angles are shown in Fig. 4 and Table 1. If the phase-matching angle is smaller than the cut angle, the minus sign of incident angle is used in Table 1, otherwise the plus sign is used. No matter the external angle is minus or plus, we have the following equations

$$K_u^2 = K_p^2 + K_{ir}^2 - 2K_pK_{ir}\cos[\pi - \theta_1 + \theta_2] \tag{1}$$

$$K_{ir}^2 = K_u^2 + K_p^2 - 2K_pK_u\cos q \tag{2}$$

$$K_u = \frac{2\pi n_u^o(\lambda)n_u^e(\lambda)}{\lambda_u\sqrt{[n_u^o(\lambda)\sin\theta_u]^2 + [n_u^e(\lambda)\cos\theta_u]^2}} \tag{3}$$

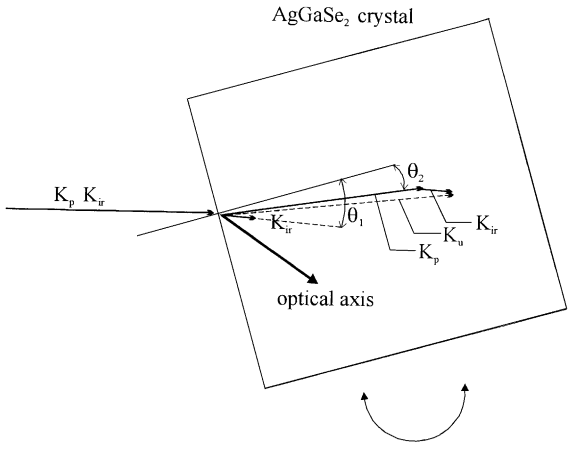

Fig. 3. The beam propagation diagram in the $AgGaSe_2$ crystal. Here the K represents wave vector. The subscripts p, ir, and u represent the OPO beam, MIR radiation and the up-converted beam generated in the $AgGaSe_2$, respectively. θ_1 is the angle between MIR radiation and the normal line of crystal. θ_2 is the angle between OPO beam and the normal line of crystal.

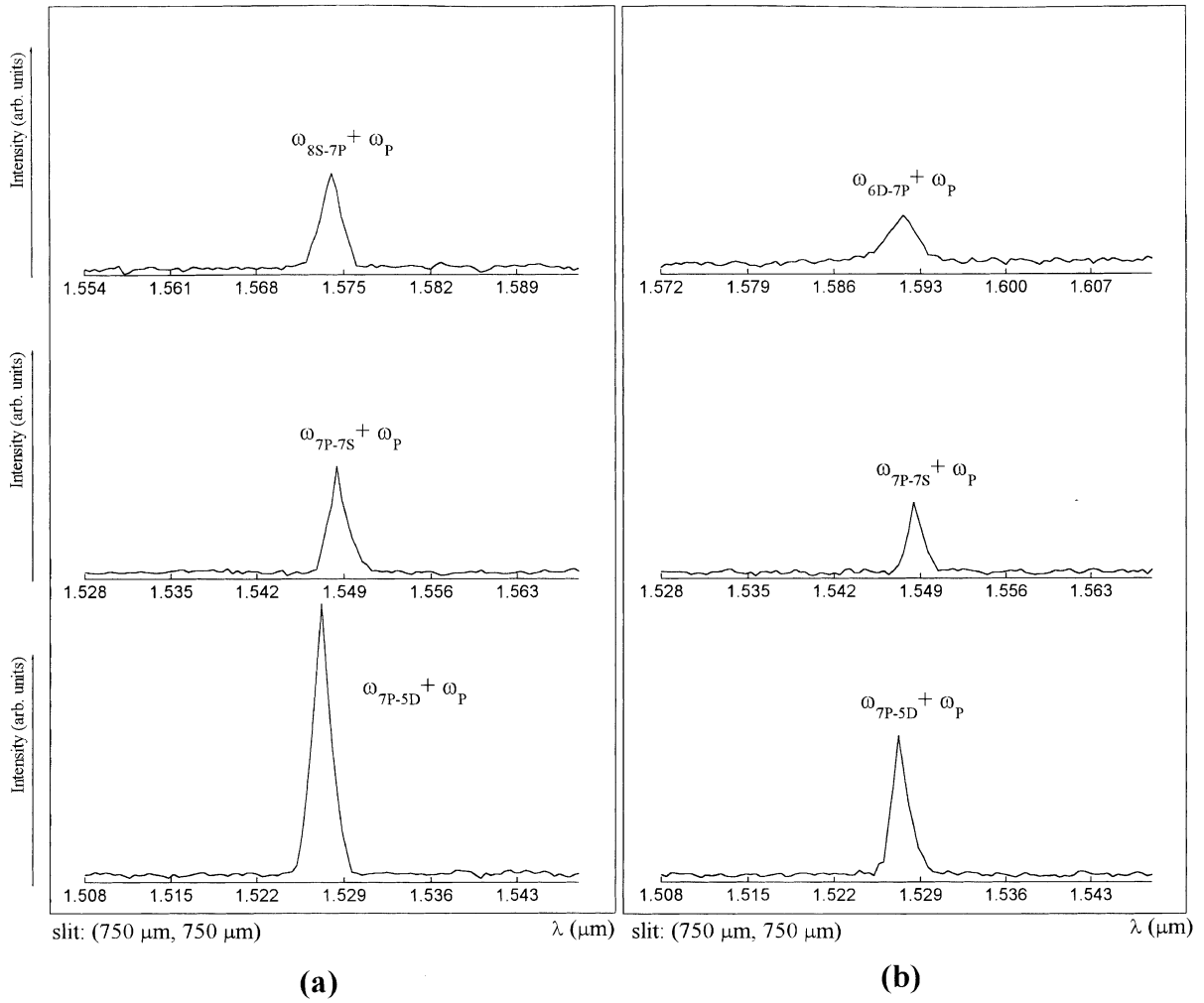

Fig. 4. The spectra measured with sum-frequency process in $AgGaSe_2$ as the potassium was excited on the (a) 4S–8S (b) 4S–6D two-photon resonance. Here the wavelength of pumping source in up-conversion process $\lambda_p(1/\omega_p)$ is 1.7870 μm.

$$K_{ir} = 2\pi n_{ir}^{e}(\lambda, \theta_{ir})/\lambda_{ir} = \frac{2\pi n_{ir}^{o}(\lambda) n_{ir}^{e}(\lambda)}{\lambda_{ir}\sqrt{[n_{ir}^{o}(\lambda)\sin\theta_{ir}]^2 + [n_{ir}^{e}(\lambda)\cos\theta_{ir}]^2}} \quad (4)$$

$$K_p = 2\pi n_p^{o}(\lambda)/\lambda_p \quad (5)$$

$$\theta_1 = \sin^{-1}[\sin\theta_E / n_{ir}^{e}(\lambda, \theta_{ir})] \quad (6)$$

$$\theta_2 = \sin^{-1}[\sin\theta_E / n_p^{o}(\lambda)] \quad (7)$$

K, λ, and n represent the wave vector, wavelength in free space, and refractive index, respectively. Superscripts o and e denote ordinary and extraordinary waves, respectively. Subscripts ir, p, and u denote the MIR radiation, OPO beam, and the up-converted beam generated in the $AgGaSe_2$, respectively. q is the angle between K_p and K_u. θ_E is the incident angle under phase-matching condition. The phase-matching angles for the MIR radiation and the up-converted signal in crystal are θ_{ir} and θ_u, respectively. The phase-matching angle can be expressed as $\theta_{ir} = \theta_c + \theta_1$ and $\theta_u = \theta_c + \theta_2 + q$, in which θ_c is the cut angle of $AgGaSe_2$. With the measurements of θ_E, λ_p, and λ_u, as shown in Table 1, the refractive indices of e-ray $n_{ir}^{e}(\lambda)$ for

Table 1
The wavelengths of MIR emissions expected to be observed, calculated and measured sum-frequency signals, and external incident angles of $AgGaSe_2$ crystal under phase-matching condition of type II

MIR wavelength predicted from the related transition λ_{ir} (μm)	Up-converted signal wavelength from the $AgGaSe_2$ λ_u (μm)		External incident angle (deg)
	Calculated	Measured	$AgGaSe_2$ (θ_E)
15.9681 $6D_{3/2}$–$7P_{1/2}$	1.5909	$1.5916 \pm 6 \times 10^{-4}$	-6.75 ± 0.5
16.0836 $6D_{3/2}$–$7P_{3/2}$	1.5920		
16.0904 $6D_{5/2}$–$7P_{3/2}$	1.5921		
14.3788 $8S_{1/2}$–$7P_{1/2}$	1.5736	$1.5740 \pm 6 \times 10^{-4}$	-4.05 ± 0.5
14.4724 $8S_{1/2}$–$7P_{3/2}$	1.5747		
12.4981 $7P_{3/2}$–$7S_{1/2}$	1.5481	$1.5484 \pm 6 \times 10^{-4}$	2.83 ± 0.5
12.5688 $7P_{1/2}$–$7S_{1/2}$	1.5492		
11.2528 $7P_{3/2}$–$5D_{3/2,5/2}$	1.5271	$1.5272 \pm 6 \times 10^{-4}$	10.83 ± 0.5
11.3101 $7P_{1/2}$–$5D_{3/2,5/2}$	1.5282		

Here the wavelength of pumping source in the sum-frequency process, λ_p, is 1.7670 μm.

Table 2
The MIR emissions and the corresponding e-ray refractive indices measured in this experiment

IR wavelength predicted from the related transition (μm)	IR wavelength measured in this work (μm)	The e-ray refractive index of $AgGaSe_2$ ($\pm 1.2 \times 10^{-3}$)
15.9681 $6D_{3/2}$–$7P_{1/2}$	$16.03 \pm 5 \times 10^{-2}$	2.517
16.0836 $6D_{3/2}$–$7P_{3/2}$		
16.0904 $6D_{5/2}$–$7P_{3/2}$		
14.3788 $8S_{1/2}$–$7P_{1/2}$	$14.41 \pm 4 \times 10^{-2}$	2.532
14.4724 $8S_{1/2}$–$7P_{3/2}$		
12.4981 $7P_{3/2}$–$7S_{1/2}$	$12.51 \pm 3 \times 10^{-2}$	2.546
12.5688 $7P_{1/2}$–$7S_{1/2}$		
11.2528 $7P_{3/2}$–$5D_{3/2,5/2}$	$11.25 \pm 2 \times 10^{-2}$	2.554
11.3101 $7P_{1/2}$–$5D_{3/2,5/2}$		

$AgGaSe_2$ in the 11–16 μm range are calculated with Eqs. (1)–(7) and listed in Table 2. Notice that the $n_{ir}^{o}(\lambda)$ in Eq. (4) is calculated with the following refractive-index Sellmeier equation for o-ray [9]

$$n_o^2 = A + \frac{B}{\lambda^2 + C} + \frac{D}{\lambda^2 + E} + F\lambda^2 + G\lambda^4 + H\lambda^6$$
$$A = 6.85472,\ \ B = 0.421498,$$
$$C = -0.168867,\ \ D = -0.000872412,$$
$$E = -2.78693,\ \ F = -0.001416,$$
$$G = 1.78628 \times 10^{-6},\ \ H = -5.78598 \times 10^{-9} \qquad (8)$$

The error of the e-ray refractive-index data listed in Table 2 are caused by the following facts: (i) the resolution of the monochromator, (ii) the uncertainty in cut angle, (iii) the uncertainty in the measurement of the external incident angle under phase-matching condition, and (iv) the uncertainty of the o-ray refractive-index data [9].

Based on our e-ray refractive-index data in the 11–16 μm range listed in Table 2 and Boyd et al.'s data in the 0.85–13.5 μm range [14], we have the following improved Sellmeier equation

$$n_e^2 = A + \frac{B}{\lambda^2 + C} + \frac{D}{\lambda^2 + E} + F\lambda^2 + G\lambda^4 + H\lambda^6$$
$$A = 6.68337,\ B = 0.45172,\ C = -0.214541,$$
$$D = -5.60471 \times 10^{-4},\ E = -2.67865,$$
$$F = -1.40695 \times 10^{-3},\ G = 1.88507 \times 10^{-6},$$
$$H = -6.55916 \times 10^{-9} \quad (9)$$

where the n_e is the e-ray refractive index and λ is the wavelength in μm. The n_e^2 curve is illustrated in Fig. 5. The standard deviation of n_e given by Eq. (9) from the source data is 2.8×10^{-4}. For comparison we calculated the e-ray refractive indices with the Sellmeier equations given by this work and Harasaki and Kato's work [13]. The results

Table 3
The refractive indices of e-ray given by our work and Harasaki and Kato for comparison

Wavelength (μm)	The e-ray refractive index for $AgGaSe_2$	
	From this work ($\pm 1.2 \times 10^{-3}$)	From Ref. [13]
11.0	2.556	2.556
11.5	2.553	2.553
12.0	2.550	2.550
12.5	2.547	2.547
13.0	2.543	2.543
13.5	2.540	2.540
14.0	2.536	2.537
14.5	2.532	2.533
15.0	2.528	2.529
15.5	2.523	2.526
16.0	2.518	2.522

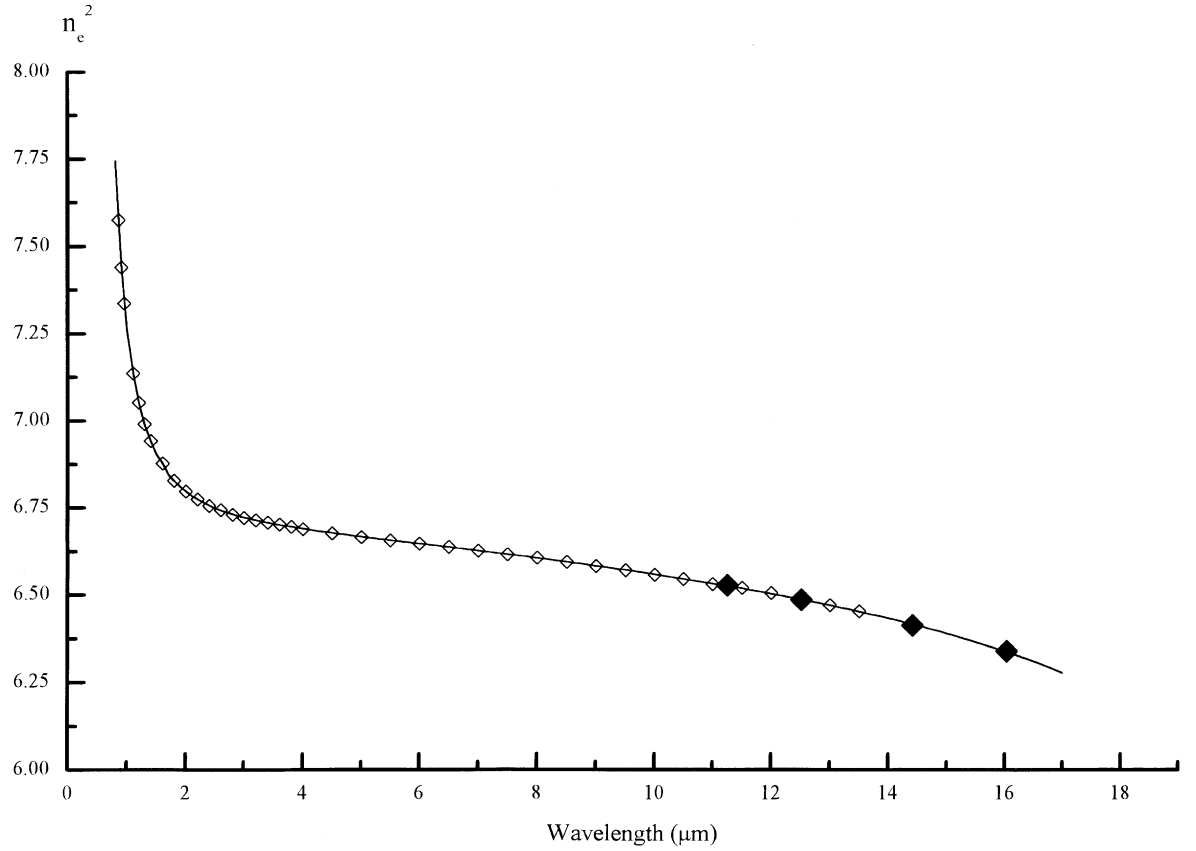

Fig. 5. The refractive-index fitting curve of e-ray for $AgGaSe_2$. The open diamond points are the experimental data reported by Boyd et al. (0.85–13.5 μm), and the solid diamond points are the experimental data measured in this work (11–16.03 μm).

are listed in Table 3. The uncertainty of the refractive-index data in this work is 1.2×10^{-3}. It can be seen that our data agree well with Harasaki and Kato's data for the wavelength shorter than 13.5 μm. However, for the wavelength longer than 13.5 μm the difference between our data and Harasaki and Kato's data grows up as the wavelength increases. According to the Harasaki and Kato's equation, the calculated external incident angle under phase matching is 2.3° larger than our measured value 6.75° at 16 μm.

This new expression (9) can be applied in the 0.85–16.03 μm wavelength range for e-ray. The two improved Sellmeier equations (8) and (9) give more accurate refractive indices than those given by Refs. [10–13] in the 13–16 μm.

4. Conclusion

In this paper, we have described a sum-frequency experiment with $AgGaSe_2$ crystal in type II configuration. Using this crystal, we measured almost all the ASE spectral lines in the 11–16 μm range at room temperature as the potassium was excited on the 4S–8S and 4S–6D two-photon resonances. We calculated the refractive indices of e-ray for $AgGaSe_2$ from the measurements of the phase-matching angles. Based on our experimental data and Boyd et al.'s data, we extend the Sellmeier equation for the e-ray refractive index to the 16 μm wavelength range. Combining this new equation with our o-ray refractive-index equation published before, these two improved Sellmeier equations can be used in the transmission range of $AgGaSe_2$ from 0.85 to 16 μm.

Acknowledgements

This project was supported by National Science Council of the Republic of China under grant no. NSC 89-2112-M-009-034.

References

[1] S.Y. Tochitsky, V.O. Petukhov, V.A. Gorobets, V.V. Churakov, V.N. Jakimovich, Appl. Opt. 36 (1997) 1882–1888.
[2] R.C. Eckardt, Y.X. Fan, R.L. Byer, R.K. Route, R.S. Feigeson, J. van der Laan, Appl. Phys. Lett. 47 (1985) 786–788.
[3] D.A. Russell, R. Ebert, Appl. Opt. 32 (1993) 6638–6644.
[4] R.C. Eckardt, Y.X. Fan, R.L. Byer, Appl. Phys. Lett. 49 (1986) 608–610.
[5] J. Kirton, Opt. Commun. 115 (1995) 93–98.
[6] K.P. Petrov, R.F. Curl, F.K. Tittel, L. Goldberg, Opt. Lett. 21 (1996) 1451–1453.
[7] K.S. Abedin, S. Haidar, Y. Kanno, C. Takyu, H. Ito, Appl. Opt. 37 (1998) 1642–1646.
[8] G.C. Bhar, S. Das, R.K. Route, R.S. Feigelson, Appl. Phys. B 65 (1997) 471–473.
[9] H.W. Wang, M.H. Lu, Appl. Phys. B 70 (2000) 15–21.
[10] H. Kidal, J.C. Mikkelsen, Opt. Commun. 9 (1973) 315–318.
[11] G.C. Bhar, Appl. Opt. 15 (1976) 305–307.
[12] D.A. Roberts, Appl. Opt. 35 (1996) 4677–4688.
[13] A. Harasaki, K. Kato, Jpn. J. Appl. Phys. 36 (1997) 700–703.
[14] G.D. Boyd, H.M. Kasper, J.H. Mcfee, F.G. Storz, IEEE J. Quant. Electron. QE-8 (1972) 900–908.